

Optimal Positioning for Energy Harvesters on a T09 AEROMAX type Aircraft's Wing

David Romero-Gonzalez
Departamento de Ingeniería
Universidad Aeronáutica en Querétaro
Querétaro, México
5419@soyunaq.mx

Javier Leal-Gutierrez
Departamento de Ingeniería
Universidad Aeronáutica en Querétaro
Querétaro, México
5305@soyunaq.mx

Oscar A. Garcia-Perez
Departamento de Ingeniería
Universidad Aeronáutica en Querétaro
Querétaro, México
oscar.garcia@unaq.mx

Abstract— The following article analyzes the optimal position for piezoelectric patches on the structure of a T09 Aeromax model aircraft's main wing to harvest the most energy possible. By analyzing the natural frequencies and their respective modal shapes with an accelerometer and real-time monitoring software, it was concluded that there are two potential locations for piezoelectric patches installation. However, this project also proposes a basis for future steps to validate these proposals and apply the energy harvested to a specific application.

Keywords—Aircraft, energy harvesting, piezoelectric patch, modal analysis.

I. INTRODUCTION

Nowadays, energy harvesting plays a crucial part in the daily products used for commercial, private, or even military applications. Some recent applications use energy harvesting for powering cities or houses using natural resources. Others use this technology as an enhancement instead of a partial replacement; for example, in F1, where with the MGU-K and MGU-H, the cars can harvest kinetic and heat energy while braking to charge their battery to pass an opponent in the future, giving them an edge over other teams. Nonetheless, the application on which this study is focused is for self-charging structures. One example of self-charging structures is load-bearing applications, as indicated by Inman & Erturk [1]. The dynamic loads suffered by the bearing are stored in thin battery layers and then reused to power other low-energy consuming systems. This analogy could be extrapolated into more advanced structures constantly subjected to higher dynamic loads, such as an aircraft's wing that suffers displacements when encountering turbulent wind gusts. The forces caused by turbulent airflow that are causing any deformation may be enough to harvest energy with a piezoelectric patch and reuse it to power low-output systems such as cabin control lights. Even though this study is limited to the positioning for these piezoelectric patches, it is necessary to detail what the applications for this researched technology might be.

Energy Harvesting

Energy harvesting can be defined as any process where energy, in any of its many states, is extracted from a system or medium and then converted (and sometimes stored) for future use [1]. One primary example is solar water heaters, where solar radiation is converted into thermal energy to heat water for household use. However, the main problem in electronic applications involving this technology is the conversion efficiency; authors Lallart & Guyomar discuss the significant losses of electrical power when converting energy into electricity [2].

Piezoelectric Effect

Certain materials have a specific property where an electric charge can be produced when mechanical stress is applied; this is called the direct piezoelectric effect, and the electric charge produced is directly proportional to the mechanical stress applied. This property allows materials to function as a communication agent between their system and surroundings, acting as sensors or actuators [3].

This property works on materials with a crystalline structure since the atoms are accommodated according to their electrical charge. This means that when mechanical stress is applied and deformation is present, the electrical balance will break, and electricity will start flowing along the structure. However, one might argue that this could happen in the opposite direction, where electricity is induced in the material, forcing it to deform its geometry; this is called the inverse piezoelectric effect [4].

Piezoelectric Patches

As previously mentioned, self-charging structures are the focus of this project. These structures have piezoelectric materials embedded along with battery layers in their structural components, so energy harvesting can occur when working under nominal conditions, taking advantage of the structure's dynamics [1]. Generally, these patches are classified for their sale according to the type of stress they will be subjected to:

- Tension
- Compression
- Flexion
- Torsion
- Shear

II. RESULTS

According to Table I, many natural frequencies with high accelerometer magnitude readings are reported, allowing any reader to assume that there is no conclusive data for a piezoelectric patch positioning. However, with the help of the real-time monitoring software Dynaview and a trustful modal analysis, it was possible to detect specific frequencies with more promising data than others. Before analyzing the results, an arbitrary WCS was proposed to express the modal shape's deformations in terms of this reference. This WCS, according to the model aircraft, is shown in Fig. 1.

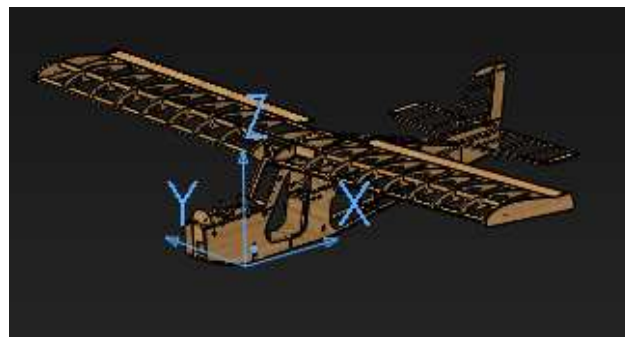


Fig. 1 Aircraft coordinate system

At first, the natural frequencies 1, 3, 9, and 10 have similar modal shapes, with a significant flexion deformation starting at the wing-fuselage joint (in the case of modal shape 3, the torsion allowed for a small amount of flexion), all deforming along the Z axis. Besides the fact that modal shapes 1 and 3 are at very low frequencies, exciting the structure would not require too much effort. Another relevant observation is that pairs 1 and 3, and 9 and 10, have their natural frequencies very close to each other, respectively. This closeness would signify that two operative frequency ranges can be described instead of having multiple functional points separated among them. This oscillation type is shown in fig. 2, showing how the aircraft demonstrated these flexional modal shapes (in numerical simulation and experimental model) when excited at frequencies 1, 3, 9, and 10. The modal shape shown is related to frequency #1 given its high FFT magnitude. However, the behavior for the other three frequencies is equal at the wing-fuselage joint.

On the other hand, Table I also shows one frequency with a significantly higher FFT magnitude than the others ($\omega_n = 46.3$ Hz). This frequency presented an FFT value of 0.160 m/s^2 representing a 196.3% above the nearest natural frequency magnitude. However, the wing's modal shape associated with this frequency has an alternating behavior along the X axis instead of vertical oscillations, as in the previous paragraph. This modal shape is shown in Fig. 2 and Fig. 3, showing the alternating oscillations in the numerical simulation and the actual model.

The other natural frequencies did not represent any outstanding or relevant data compared to the abovementioned cases.

One relevant piece of information can also be shown in Table I, where the most contributive axis is presented for each modal shape. This axis is related to the orientation that the model aircraft was subjected to vibrations, not the resulting deformations.

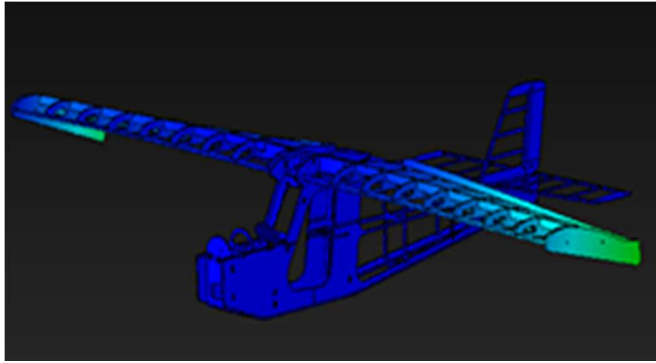


Fig. 2 Numerical modal analysis

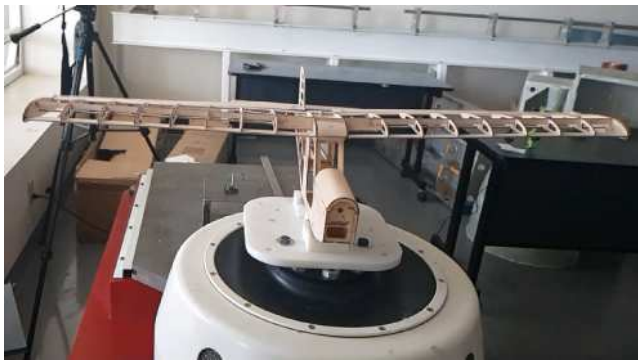


Fig. 3 Experimental modal analysis



Fig. 4 Fifth experimental modal shape

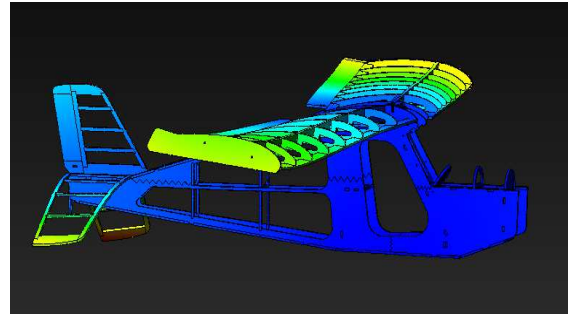


Fig. 5 Fifth Numerical Modal Shape

TABLE I. T09 Aeromax natural frequencies and modal shapes

Mode Shape	Frequencies [Hz]		
	ω_n	FFT Magnitude [m/s^2]	Most contributive axis
1	12.2 Hz	0.055	Y
2	17.7 Hz	0.020	Z
3	24.9 Hz	0.0325	Y
4	32.6 Hz	0.010	Z
5	46.3 Hz	0.160	X
6	60.0 Hz	0.019	Y
7	68.9 Hz	0.054	Z
8	70.2 Hz	0.054	Y
9	76.1 Hz	0.014	Z
10	89.8 Hz	0.040	Z

The first proposal with more promising results is according to the analysis of the first results presented in the previous section. The piezoelectric patch would have to be mounted on the wing-fuselage joint along the wing's top surface, as shown in Fig. 6. The main reason behind this location is for having many natural frequencies with relative ease of excitement. It is important to notice that Fig. 5 shows the deflections on the wing for an easier understanding of the location proposal. However, considering that the patches are stress-dependent coerces the location to be on the joint where the stress is concentrated.

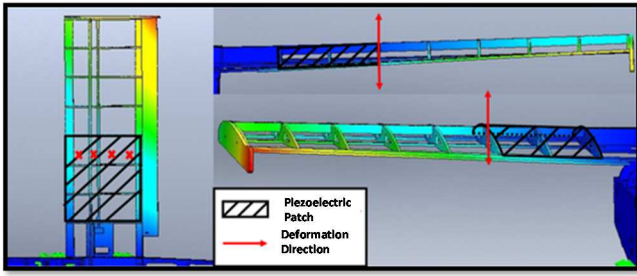


Fig. 6 First proposal for piezoelectric patch positioning on wing

The second proposal stands afterward, given its occurrence; it only presented its modal shape one time along the spectrum. However, given that it presents a great deformation relative to the other modal shapes, it is hypothesized to have an area with more kinetic energy available to harvest. Instead, the location would be inside the wing's structural beam to receive the X-axis deformations for energy harvesting. This proposal is shown in Fig. 7. Similar to the first proposal, stress is concentrated on the joint between the wing and fuselage, influencing the positioning in the same manner.

It is essential to mention that when selecting the patch to be installed the mean stress and maximum stress on the joint must be calculated and considered so that the patch may resist and function properly. If the patch suffers stresses and fatigued beyond its design limits it will probably fail and break, while if a sturdier patch is installed additional unnecessary weight and stiffness will be acting upon the wing and considerably changing its dynamic response. Either way, indirect damping will be added given that the mechanical energy inputting, dissipating, and redirecting this energy in order for it to be converted into electrical energy.

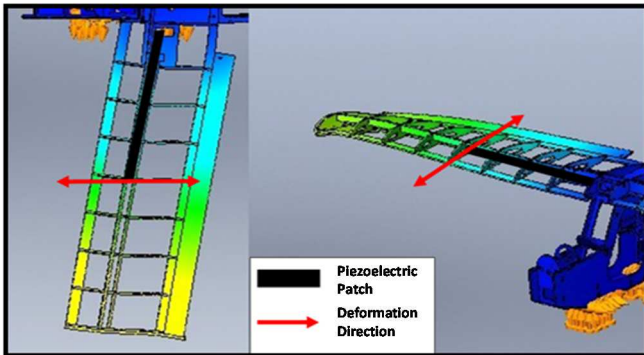


Fig. 7 Second proposal for piezoelectric patch positioning on wing

III. CONCLUSIONS

The main advantage of these proposals is that the piezoelectric patch will be for flexion, allowing for a selection of a flexion-type patch. The different proposals would have the same type of piezoelectric patch only differing on the orientation and positioning. However, it is impossible to theorize which proposal will work the best, given that the modal analysis conducted did not represent any aeroelastic deformations. To conclude precisely which proposal is best, a dynamic aeroelastic study must take place to see which proposal excites the model aircraft with more kinetic energy in nominal flight conditions. There is also the possibility of having these two proposals discarded, given that the aeroelastic deformations do not always coincide with the static analysis; however, this study does deliver promising results for future analysis. This last conclusion would open the next phase for research on this model aircraft, reviewing the deformations presented at take-off, cruise flight, and landing. Another opportunity for improvement could be adding combined vibration orientations; some axis contributed more than others in some modal shapes shown in Table II. It is possible to have new modal shapes because of

combining two or more vibration orientations which would, in turn, open space for analyzing the optimal positioning for piezoelectric patches on the wing.

Regarding the installation of a piezoelectric patch, the structure's natural damping behavior will probably be affected, mainly due to the mechanical energy being converted into electrical energy acting as an indirect damping element. Moreover, only structural damping was considered, thus by including all the additional damping factors the vibrations produced on the wing will probably stay in a certain amplitude range. In terms of the natural frequency, these frequencies might probably shift; however, only the modal shapes determine the patch's position, meaning this frequency shift is not relevant.

TABLE I. Description T09 Aeromax natural frequencies and modal shapes

Modal Shape	Description
1	Location: Antinode at wing's trailing edge on the main wing tip. Displacement: Alternating movement between semi-spans; flexion with a slight torsion relative to the Z axis as shown in Fig 8.
2	Location: Antinode at wing's trailing edge on the main wing tip. Displacement: Simultaneous movement between semi-spans; flexion with slight torsion relative to the Z axis as shown in Fig 9.
3	Location: Antinode at wing's trailing edge on the main wing tip. Displacement: Alternating movement between semi-spans; torsion relative to the XZ plane and slight flexion relative to the Z axis as shown in Fig 10.
4	Location: Antinode at wing's trailing edge on the main wing tip. Displacement: Simultaneous movement between semi-spans; torsion relative to the XZ plane as shown in Fig 11.
5	Location: Antinode at main wing & horizontal stabilizer's wing tips. Displacement: Main Wing (Most predominant) - Simultaneous movement between semi-spans; flexion relative to the X axis. Horizontal Stabilizer: Simultaneous movement between semi-spans; flexion relative to the Z axis as shown in Fig 5.
6	Location: Antinode at horizontal & vertical stabilizer's wing tips. Displacement: Horizontal Stabilizer - Alternating movement between semi-spans; flexion relative to the Z axis. Vertical Stabilizer (Most Predominant): Moderate oscillating flexion relative to the Y axis as shown in Fig 12.
7	Location: Antinode at main wing & horizontal stabilizer's wing tips. Displacement: Main Wing - Simultaneous movement between semi-spans; flexion relative to the X axis. Horizontal Stabilizer (Most predominant) : Simultaneous movement between semi-spans; flexion relative to the Z axis as shown in Fig 13.
8	Location: Antinode at horizontal & vertical stabilizer's wing tips. Displacement: Horizontal Stabilizer - Alternating movement between semi-spans; flexion relative to the Z axis. Vertical Stabilizer - Moderate oscillating flexion relative to the Y axis as shown in Fig 14.
9	Location: 2 Antinodes; first one located at one-third distance of the semi-span's trailing edge. Second one located at the wing's tip trailing edge. Displacement: Alternating movement between semi-spans; flexion relative to the Z axis. Main torsion at the semi-spans created by the antinode displacements. Highest displacement at right semi-span section.
10	Similar displacement as the previous modal shape with the distinctions that the movement is simultaneous instead of alternating between semi-spans and that the most main displacement is located at the left semi-span.

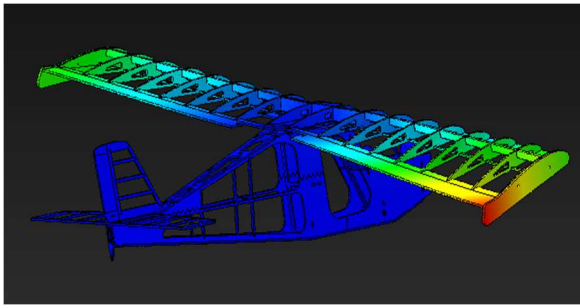


Fig. 8 First modal shape

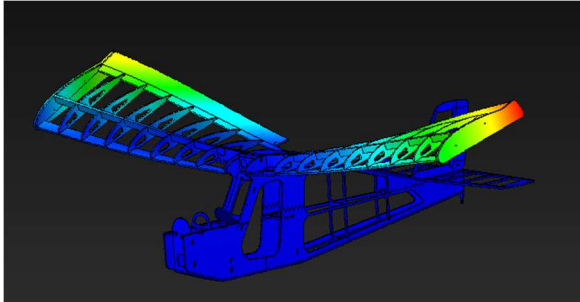


Fig. 9 Second modal shape

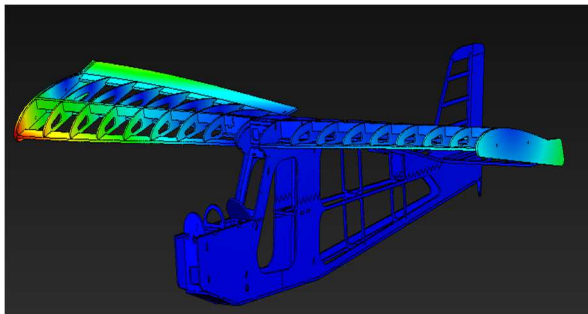


Fig. 10 Third modal shape

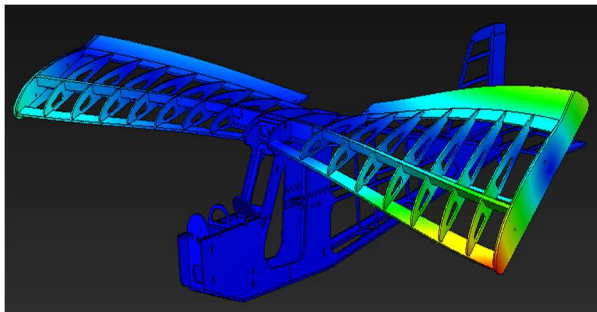


Fig. 11 Fourth modal shape

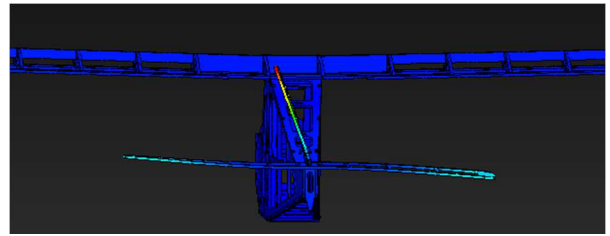


Fig. 12 Sixth modal shape

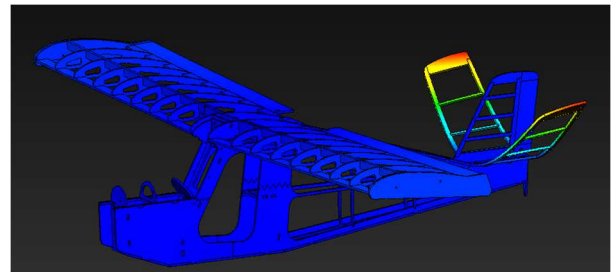


Fig. 13 Seventh modal shape

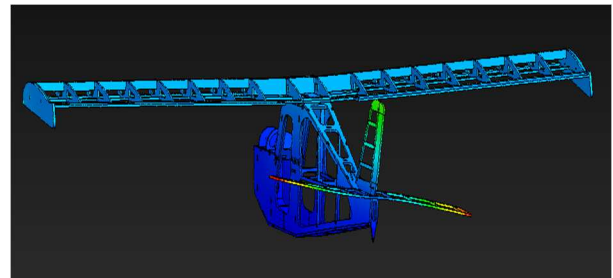


Fig. 14 Eight modal shape

REFERENCES

- [1] A. Erturk & D. J. Inman, Piezoelectric Energy Harvesting, West Sussex: Wiley, 2011.
- [2] M. Lallart and D. Guyomar, "An optimized self-powered switching circuit for non-linear energy harvesting with low voltage output", Smart Materials and Structures, 2008, vol. 17, no 3.
- [3] K. Uchino, "The Development of Piezoelectric Materials and the New Perspective", the Advanced Piezoelectric Materials, Philadelphia, Woodhead Publishing, 2010, pp. 1-92.
- [4] C. Fleischer, "Feel the Squeeze: How Piezoelectricity Works to Make Crystals Conduct Electric Current", Autodesk.com <https://www.autodesk.com/products>. (accessed: January 25, 2022)